

Recombination of dyons into calorons in $SU(2)$ lattice fields at low temperatures

E.-M. Ilgenfritz^a, B. V. Martemyanov^b, M. Müller-Preussker^a
and A. I. Veselov^b

^a Humboldt-Universität zu Berlin, Institut für Physik, D-12489 Berlin, Germany

^b Institute for Theoretical and Experimental Physics, Moscow 117259, Russia

December 2, 2024

Abstract

By cooling of equilibrium lattice fields at finite temperature in $SU(2)$ gauge theory it has been shown that topological objects (calorons) observed on the lattice in the confined phase possess a dyonic substructure which becomes visible under certain circumstances. Here we show that, with decreasing temperature of the equilibrium ensemble, the distribution in the caloron parameter space is modified such that the calorons appear non-dissociated into constituent dyons. Still the calorons have nontrivial holonomy which is demonstrated by the Polyakov line behaviour for these configurations. At vanishing temperature (on a symmetric lattice) topological lumps obtained by cooling possess rotational symmetry in $4D$ and a characteristic double peak structure of Polyakov lines (defined with respect to temporal and spatial directions) with non-trivial asymptotics.

1 Introduction

At high temperatures, near but below the deconfinement temperature, classical solutions of Yang-Mills equations with nontrivial holonomy (KvB calorons [1, 2]) are seen on the lattice for $SU(2)$ gauge theory to be frequently dissociated into dyons [3, 4, 5, 6]. This means that the distance between the dyons forming a caloron,

$$d = \frac{\pi \rho^2}{b} , \tag{1}$$

is larger than the size of dyons (b/π for the case of maximally nontrivial holonomy). Here ρ is the instanton size parameter and b is the temporal periodicity interval.

These observations have been made by the use of cooling. Therefore the question arises why such a substructure never has been observed by previous authors who have used the cooling method. In this paper we will argue that there is only a certain window of temperature where it can be revealed by this method.

The interest in the existence of caloron constituents has increased since it has been demonstrated in Ref. [7] that a constituent substructure very reminiscent of the caloron solutions can also be identified without cooling, above and below the phase transition. This can be achieved by using the localization properties of the fermionic zero modes of a suitably chirally-improved Dirac operator. The similarity with the properties of a caloron solution is realized for a certain fraction of $Q = \pm 1$ configurations, where the single zero mode is seen to change its localization when the periodicity of fermionic boundary conditions becomes modified. A systematic study [7] of the typical pattern of localization and delocalization followed by jumps of the zero mode has revealed that this pattern depends on the timelike holonomy exactly in a caloron-like way. Whereas the topological density has a much more complicated structure, the positions where the zero mode is pinned-down actually show the signatures expected for caloron constituents [8]: these are local maxima of the topological density $q(x)$ with a sign as required by the chirality of the mode. This suggests that (dissociated or non-dissociated) calorons might really form the semiclassical background of the gauge field near the phase transition.

Coming back to $SU(2)$ calorons with their two constituents, it seems that the quantities d and ρ appearing in eq. (1) are impossible to be measured simultaneously: when d is seen by observation of separate dyon positions no instanton-like profile (of topological density) is observed which could be used to define ρ . When d goes to zero ($d \ll b$) an instanton size parameter ρ *can be measured* by comparison with the instanton's action density profile, but then *no dyons are seen* as separate objects. More precisely: the parameter d cannot be measured for *all* caloron configurations as the distance between constituents as long as only the action or topological charge densities are available as local observables to describe them.

The time periodicity parameter b defines the temperature T : $b = 1/T$. In order to demonstrate how the recombination of constituents depends on the temperature we can change it by varying b , *i.e.* the temporal extent of the lattice.

The paper is organized as follows. In section 2 we draw the attention to the static nature of configurations near the deconfining transition. Section 3 presents our results on semiclassical configurations at finite temperatures, pointing out the loss of "staticity" and the increasing importance of the Polyakov loop for detecting the non-trivial substructure at lower temperature. In section 4 we extend the cooling studies to the symmetric torus. We emphasize the principal inadequacy of the KvB caloron solutions extended to this case, although also this solution would consist of recombined dyonic constituents. Finally, in section 5, we discuss the consequences, also in the perspective of a twin paper by Gattringer *et al.* .

2 Non-staticity and separation into constituents

It turns out that the possibility to observe the dyonic constituents of a KvB caloron as lumps of action depends on $(\frac{\pi\rho}{b})^2$. In $SU(2)$ LGT at $\beta = 2.2$ on a lattice $16^3 \times 4$ the parameter ρ is concentrated near the value $\rho \approx 2.5a$ (a is the lattice spacing) [4]. With $b = 4a$,

$$(\frac{\pi\rho}{b})^2 \approx 4 \gg 1.$$

This means that dyons are well separated. The value of ρ in [4] was determined by fitting the lattice caloron with the analytic KvB caloron, and formula (1) was used. On the lattice $16^3 \times 6$ (with $b = 6a$) and at the same $\beta = 2.2$ (*i.e.* at a temperature 1.5 times lower) the parameter $(\frac{\pi\rho}{b})^2$ would be of the order $O(1)$. Then, from this simple arithmetics, one would expect that calorons are not dissociated into dyonic lumps anymore.

The possibility to measure the distance between dyons inside a caloron just by detecting the peaks of the action density on the lattice is given only in the case of well-separated objects. Indirectly this distance can be measured by measuring a quantity that can be called non-staticity¹. For an analytic KvB caloron with given holonomy there is a one-to-one correspondence between the distance and non-staticity. Unfortunately, cooling yields metastable plateaus only for temperatures below the deconfining temperature. On the other hand, this allows us to restrict ourselves in the following to maximally non-trivial holonomy, when the average Polyakov line vanishes. To describe in this situation the relation between distance d and non-staticity, we have considered analytical caloron solutions in continuous space-time. Then we divided the time interval b into N_t time slices and expressed the action in the i -th time slice, $S_i = \sum_{\vec{x}} s_{\vec{x},i}$, in terms of the local action density $s_{\vec{x},i}$. The non-staticity δ_t is defined as

$$\delta_t = \frac{\sum_{i=1}^{N_t} \sum_{\vec{x}} |s_{\vec{x},i+1} - s_{\vec{x},i}|}{\sum_{i=1}^{N_t} \sum_{\vec{x}} s_{\vec{x},i}}. \quad (2)$$

Obviously, this definition depends on the number of time slices N_t such that one would have $\delta_t \rightarrow 0$ for $N_t \rightarrow \infty$. In order to get an asymptotically N_t independent quantity we will modify the definition of δ_t as follows

$$\delta_t = \frac{\sum_{i=1}^{N_t} \sum_{\vec{x}} |s_{\vec{x},i+1} - s_{\vec{x},i}|}{\sum_{i=1}^{N_t} \sum_{\vec{x}} s_{\vec{x},i}} \frac{N_t}{4}. \quad (3)$$

The factor $1/4$ has been chosen such that for a lattice $16^3 \times 4$, where all the simulations were initially done using (2), the two definitions (3) and (2) agree.

With the definition (3) at hands we can calculate the non-staticity of an analytic KvB caloron. The non-staticity depends on the holonomy and on the distance between the constituents inside the caloron. For maximally nontrivial holonomy (coinciding with the average holonomy in the confinement phase) the constituent dyons have equal mass.

¹See Ref. [6] where it has been defined in a slightly different way.

For this generic case we have determined a bifurcation value of the non-staticity, $\delta_t^* = 0.27$, choosing the distance between the constituents such that the two lumps of action density (dyons) merge into one lump of action density. This single lump is what we call a "recombined caloron". As already mentioned, the non-staticity uses the discreteness of a lattice configuration. The value δ_t^* is obtained by inserting the analytic form of the action density of a continuum KvB caloron solution [1], calculated exactly at the point of bifurcation, into the evaluation of (3) using a grid with lattice spacing $a = b/N_t$. In order to see how well-defined at finite N_t this "bifurcation value" δ_t^* can be, we have evaluated it for various (even and odd) $N_t \geq 4$. The function $\delta_t^*(N_t)$ that goes to $\delta_t^* = 0.27$ for $N_t \rightarrow \infty$ is presented in Fig. 1.

If the non-staticity is lower than the bifurcation value δ_t^* two dyons can be distinguished by the two maxima of the action density. If the non-staticity is bigger than δ_t^* two dyons appear recombined into a caloron with only one action density maximum.

3 Recombination of dyons into calorons with lowering temperature

The results of this paper represent ensembles of about 8000 independent $SU(2)$ gauge field configurations created by heat bath Monte Carlo at $\beta = 2.2$ with respect to the Wilson action S_W on lattices $16^3 \times N_t$ with $N_t = 4$, $N_t = 5$ and $N_t = 6$. Cooling of these configurations was performed using the fastest possible relaxation with respect to the Wilson action. For this method each link $U_{x,\mu}$ is immediately replaced by the projection to $SU(2)$ of the staples around it, $\tilde{U}_{x\mu}$.

The cooled configurations studied in this paper have been identified when the cooling history passes a plateau on the level of the action of a single instanton ², $S_W \approx S_{inst} = 2\pi^2$. More precisely, the stopping criterium for cooling was that the violation of the lattice equations of motion [6] passes through a minimum. Here, the violation is defined as

$$V = \sum_{x\mu} \left(\frac{1}{2} \text{tr} [U_{x\mu} - \tilde{U}_{x\mu}]^\dagger [U_{x\mu} - \tilde{U}_{x\mu}] \right)^{1/2}. \quad (4)$$

In addition to that, the following conditions have been imposed for the selection of classical solutions :

- the decrease of action has slowed down to $|\Delta S_W|/S_{inst} < 0.05$,
- the action fits into the window $0.5 < S_W/S_{inst} < 1.25$ and
- the violation of the equations of motion, $V < 25$.

Without this last condition, we would find a broad gap between "good solutions" with $V < 20$ and "fake solutions" with very big violation. ³ The efficiency of these conditions

²At the end we describe also some results concerning higher plateaux of action, $S_W \approx 3S_{inst}$.

³These criteria have been tested for $N_t = 4$ and applied also to $N_t = 5$ and 6 (at the same β).

was such that 80 % ($N_t = 4$), 60 % ($N_t = 5$) and 55 % ($N_t = 6$) of the equilibrium configurations ended up in a cooled configuration at the one-instanton plateau. These are the classical caloron configurations which are described in the following with respect to their dyonic properties.

We remind the reader that the recombination threshold $\delta_t^* = 0.27$, strictly speaking, reflects the recombination for maximally non-trivial holonomy only, *i.e.* with an asymptotic value of the Polyakov line $L_{as} = 0$. If one performs cooling without special restrictions concerning the holonomy, there is no guarantee that the asymptotic holonomy of the caloron configurations still coincides with the average Polyakov line of equilibrium configurations in confinement. For the purpose of defining an *asymptotic* holonomy L_{as} for each cooled configuration, we have determined the average of $L_{\vec{x}}$ over a 3D subvolume where the local 3D action density $s_{\vec{x}}$ is low, for definiteness $s_{\vec{x}} < 0.0001$. In Fig. 2 we present the distribution of cooled configurations over L_{as} as a histogram (with bin size 0.1) for the three cases $N_t = 4$, $N_t = 5$ and $N_t = 6$. In the legend we show the respective volume fraction ($F \approx 0.15$) of the three-volume (*i.e.* far from the lumps of action and topological charge) over which the "asymptotic" value L_{as} is defined as an average.

As explained above, the non-staticity δ_t is a measure which describes the distance from a perfectly (Euclidean) time independent configuration. In other words, the distributions of non-staticity of caloron events obtained by cooling of equilibrium lattice configurations can be considered as a substitute for the distribution in dyon distances d . This quantity can be directly measured for cooled lattice gauge field configuration. We show the δ_t distributions for all our cooling products obtained at $\beta = 2.2$ on $16^3 \times N_t$ lattices in Fig. 3.

In an attempt to make a fair comparison with calorons with non-trivial holonomy and to correct for the possible evolution of the asymptotic holonomy away from $L_{as} = 0$ during the cooling process, we defined a subsample by the requirement $|L_{as}| < 1/6$. One can see that the cut with respect to the asymptotic holonomy selects cooled configurations from the flat central part of the histogram shown in Fig. 2. On the other hand, we notice that a considerable fraction of cooled configurations has developed an asymptotic holonomy $|L_{as}| > 1/6$.

In Fig. 3 (a) we show the probability distribution over δ_t for cooled configurations with an action at the one-instanton plateau without the cut according to the asymptotic holonomy $|L_{as}|$. One can see that a relatively high fraction of configurations, obtained from the Monte Carlo equilibrium with $N_t = 4$, has $\delta_t < \delta_t^* = 0.27$. This means that they would be identifiable as consisting of two constituents by looking for the 3D action density on the lattice. For $N_t = 5$ it is only a minority of cooled configurations which falls below the threshold $\delta_t = 0.27$. No static (according to the non-staticity criterium) configurations have been found among cooling products at $N_t = 6$.

We have repeated the same analysis after applying the cut with respect to the asymptotic holonomy, $|L_{as}| < 1/6$. Then we get modified histograms in δ_t for the three temperatures. This is shown in Fig. 3 (b). The histograms got more pronounced peaks in δ_t which are positioned around 0.125, exactly around $\delta_t^* = 0.27$, and around 0.5 for $N_t = 4$, $N_t = 5$ and $N_t = 6$, respectively.

There are other criteria which could be used to characterize a more or less static configuration, for example, the presence of static Abelian monopoles emerging in the maximal Abelian projection. This criterium is not identical with the separation set by δ_t^* . Thus, another subsample can be defined by the property that a pair of static Abelian monopoles has been found after fixing the cooled configuration to the maximal Abelian gauge and doing the Abelian projection. This subsample can be analyzed with respect to the three-dimensional distance R between the Abelian monopoles.

In Fig. 4 (a) we show the histogram over δ_t of all cooled configurations obtained from the Monte Carlo ensemble at $N_t = 4$ together with the histogram of those which explicitly exhibit the dyon-dyon structure in terms of Abelian monopoles. One can see that practically all cooled configurations below δ_t^* possess this structure, but above δ_t^* the fraction rapidly goes to zero. We show the same for $N_t = 6$, *i.e.* at lower temperature, in Fig. 4 (b). In this case, at the peak value around $\delta_t = 0.5$ only 20 % of the solutions still are characterized by a static dyon-dyon pair, whereas at higher non-staticity this is never the case. In these two distributions no cut with respect to the asymptotic holonomy has been applied.

Up to now we have two tentative definitions of the position of the constituents: one is the position of the two static Abelian monopoles (in MAG, as long as they are static) and the other is defined by the maxima of the $3D$ action density.⁴ In the case of well-separable maxima of the latter these maxima fall close to the positions of the MAG monopoles. In the other limiting cases of recombined maxima or imbalanced (this corresponds to an asymptotic holonomy far from zero) maxima of the $3D$ action density the absolute maximum is still easy to find. It is the single maximum or takes the role of one of the maxima. For the case of $N_t = 4$, *i.e.* the temperature just below deconfinement, we show in Fig. 5 (a) the histogram with respect to the local Polyakov loop at the two sorts of $3D$ constituent points, the loci of static monopoles or the maximum of action density. In both definitions the histogram peaks near to $L_{\vec{x}} = \pm 1$. The peak is however more pronounced for the monopole locations, less pronounced for the maxima of the $3D$ action density.

The relation between the non-staticity δ_t and the distance R between the static dyonic constituents emerging (in MAG as Abelian monopole) given in lattice units, is presented in Fig. 5 (b) for the higher temperature, near the deconfinement temperature ($N_t = 4$). For this temperature such dyon-dyon events are clearly distinguishable among the cooled configurations as long as the non-staticity $\delta_t < 0.6$. For extremely low non-staticity δ_t (left from the peaks in Fig. 3 (a) and (b)) we find an average distance $R \approx 7$, whereas near δ_t^* the average distance is $R \approx 4$. For higher δ_t , the part of solutions which still possesses a clear dyon-dyon structure in terms of Abelian monopoles, has them localized at distances R between one and two lattice spacings.

In order to represent how the Polyakov line behaves inside a lump of action, we have explored the neighborhood of the absolute maximum of the $3D$ action density (denoted

⁴For the case of analytical caloron solutions, the relation between the constituent locations, the locations of the maxima of the action density and the locations where $|P| = 1$ has been compared in Ref. [9].

as central point \vec{x}_0). This position could either be one of the two dyonic lumps (as long as they are separable) or the center of a "recombined" caloron. For this purpose, we have defined a locally summed-up Polyakov line L_{tot} (summed over the central point \vec{x}_i ($i = 0$) and its six nearest neighbors \vec{x}_i ($i = 1, \dots, 6$):

$$L_{tot} = \sum_{i=0}^6 L_{\vec{x}_i} \quad (5)$$

and a kind of Polyakov-line dipole moment over the same set of 3D lattice points with respect to the central point:

$$\vec{M}_{tot} = \sum_{i=1}^6 L_{\vec{x}_i} (\vec{x}_i - \vec{x}_0) . \quad (6)$$

The absolute value $|L_{tot}|$ of the first quantity tests the amount of local coherence of the Polyakov line. The absolute value $|\vec{M}_{tot}|$ of the second quantity tests the amount of presence of opposite-sign Polyakov lines representing eventually two different constituents inside the same lump of action. Fig. 6 (a) shows how the $|L_{tot}|$ (*i.e.* the locally summed-up Polyakov line) changes with δ_t in different bins of width 0.1. For the temperature nearest to the transition, at $N_t = 4$, we see that $|L_{tot}|$ falls from ≈ 4.0 to ≈ 1.0 at $\delta_t \geq 0.5$. We interpret this such that in the region, where constituents can be well separated according to the action density (at small δ_t), they are characterized by a relatively smooth change of the Polyakov line inside. In the region of large δ_t where they are not separable according to the action density, the Polyakov line changes rapidly in the neighbourhood of the absolute maximum of action density. For the lower temperatures, $N_t = 5$ and $N_t = 6$, the relationship between these properties of an action cluster and δ_t is the same, however, separable lumps of action (at low δ_t) become very rare. Fig. 6 (b) shows how the "dipole moment" $|\vec{M}_{tot}|$ of the Polyakov line around a maximum of action density rises with increasing non-staticity δ_t . In the region where one can separate the constituents according to the action density, the dipole moment is small, emphasizing again the homogeneity of the Polyakov line around the central point. In the region beyond δ_t^* the dipole moment gradually stabilizes around a value of 1.5.

In the same way as described so far, we have analyzed configurations obtained by cooling at higher action plateaux. As an example we show in Fig. 7 the histogram of non-staticity δ_t for the same three temperatures represented by $N_t = 4$, $N_t = 5$ and $N_t = 6$. Although the precise border between static and non-static has not the clear meaning as for the one-caloron case, the trend is the same: at lower temperature the lumps of action tend to be more localized also in Euclidean time ("instanton-like"). Compared with the one-caloron case, the histograms are more smeared.

4 Instantons or calorons on a symmetric 4-torus

We have also cooled equilibrium configurations generated with $\beta = 2.2$ on symmetric lattices (16^4 representing "zero" temperature). In this case we have found for the clas-

sical configurations at the plateau $S_W \approx S_{inst}$ a broad distribution of non-staticity with a maximum around $\delta_t \approx 2$ and with a tail extending beyond 3. These are obviously configurations with an action (topological charge) density well-localized in all four Euclidean directions. There is a non-trivial behaviour of the Polyakov line inside these non-dissociated, instanton-like objects resembling that which has been seen in the finite temperature case for non-dissociated calorons, however only in the Polyakov line associated with the time direction. We have mapped the cooled lattice configuration with the help of all 4 possible definitions of Polyakov line, which are physically equivalent to each other on a symmetric lattice. Fig. 8 shows the profiles of action density, topological charge, and of the Polyakov lines (for four possible definitions) as they are seen in appropriate planes intersecting the lump through the centrum. The latter is defined as the maximum of the 4D action density. For all types of Polyakov lines the characteristic double peak structure is seen exactly when the "asymptotic" value of the respective Polyakov line is *not close* to ± 1 .

It is interesting to compare the pattern of the Polyakov line of these "caloron candidates" with the analytic KvB caloron formally constructed on a 16^4 lattice corresponding to maximally non-trivial holonomy with respect to a chosen "time" direction. For this construction, the two constituents have been placed along the z -direction, separated by 8 lattice spacings. The lattice caloron is obtained calculating link by link from the continuum gauge field A_μ . Of course, such a constructed lattice caloron has irregularities at the boundary if the lattice action is evaluated under the assumption of periodicity. After some cooling the configuration turns into an (approximate) solution of the lattice equations of motion *on the torus*. By that time the boundary artefacts have disappeared, see Fig. 9, *i.e.* the KvB caloron is adjusted to periodic boundary condition also in the x, y, z - directions and the Wilson action has become $S_{inst} \approx 2\pi^2$. Despite the large separation the constituents formally have, judging according to the action density it appears as a non-dissociated instanton. It is seen that the cooling does not influence significantly the structure of the Polyakov lines of the KvB caloron, and only the time-directed Polyakov line (plt) shows the double peak structure mentioned above, while the space-directed Polyakov lines (plx, ply, plz) have a simple structure characteristic for trivial holonomy. It is analytically clear that for caloron solutions asymptotically $plx, ply, plz \rightarrow \pm 1$. This is in contrast to the would-be "caloron candidate" obtained by cooling from confining equilibrium lattice configurations at zero temperature (Fig. 8) where the double peak structure can be present for all (t, x, y, z) directions when, generically, the asymptotic holonomy in the corresponding directions is non-trivial.

5 Conclusions and perspectives

In the present investigation we have subjected equilibrium lattice gauge fields at various temperatures to ordinary relaxation called "cooling" in order to strip off quantum fluctuations. In this way we have extracted lowest-action classical solutions of unit topological charge typical for the given equilibrium ensemble. Notice that, at least as long this tech-

nique is used, this possibility is restricted to the confinement phase. We do not claim to find the real and complete topological structure hidden under the quantum fluctuations and consisting of topological lumps of compensating sign. What we wanted to see were the simplest solutions suitable as a principal starting point for a semi-classical modelling of the Yang-Mills path integral. In conclusion we can say, that cooling of equilibrium lattice fields in $SU(2)$ lattice gauge theory shows that there exist topological objects with a dyonic substructure, that we are able to resolve only in the confined phase. With decreasing temperature it becomes more likely that the observed dyons recombine into calorons such that it becomes impossible to perceive the substructure looking *only* at the distribution of action and topological charge. Still, these calorons have a nontrivial holonomy which is mapped out by the behavior of the Polyakov line *inside and outside* these configurations.

In the limiting case of zero temperature (*i.e.* on a symmetric lattice) $Q = \pm 1$ topological lumps obtained by cooling look instanton-like and, at the same time, have the characteristic double peak structure of the Polyakov line defined *all* t, x, y, z directions where it, generically, behaves asymptotically non-trivial. This distinguishes them from the real KvB solutions which possess a distinguished "time" direction.

Although, strictly speaking, an analytic solution of the Euclidean equations of motion with $Q = \pm 1$ is impossible on the $4D$ torus [10], on the lattice quasistable solutions of this kind exist. If considered only as lumps of action and topological charge, there is no contradiction with the previous observations from "instanton searches". As our analysis shows, for temperatures much lower than the deconfinement temperature rotationally symmetric (in $4D$) and (anti)selfdual lumps seem to be preferred under cooling.

At finite temperature, they can be subsumed under the general class of KvB solutions. For zero temperature, however, a so far unknown parametrization corresponding to non-trivial asymptotic holonomy has to be found.

After having completed the present investigation we were informed by Ch. Gattringer and R. Pullirsch [11] about their paper "Topological lumps and Dirac zero modes in $SU(3)$ lattice gauge theory on the torus" prior to publication. In this paper the authors concentrate on and more systematically continue the inspection of the low-lying modes of the chirally improved Dirac operator on the 4-torus, in the background of equilibrium lattice gauge fields at $T = 0$. It is extremely interesting that they find, for a certain fraction of Monte Carlo configurations in the $|Q| = 1$ sector, a similar pattern of hopping zero-modes as a function of varying fermionic boundary conditions. Moreover, the change of localization happens independently of which out of the four directions is chosen as "imaginary time" direction along which periodicity can be purposedly changed. The concurrent zero mode positions (two or three as in the finite temperature case) are consistent with being randomly distributed in the $4D$ periodic box. The authors argue that this observation hints at the existence of a semiclassical background consisting of localized (in $4D$) instanton constituents. Whereas other (monopole ?) properties of the constituents are less obvious, a non-integer topological charge of the constituents has been hypothetically assumed in analogy with the dissociated KvB solutions. In fact, this should not be too difficult to be established. It is in particular this last interpretation that has to pass further tests. In case it becomes confirmed then it would be difficult to reconcile this with

our observations based on cooling. Our findings are consistent with a picture in which (at finite temperature) the temporal size of the box determines (inversely) the size of the background solutions. In contrast, the scenario of Ref. [11] seems to imply a complete dissolution (within the available 4-volume) of some constituents which still span a coherent semiclassical background. This would mean that there is no scale of coherence which is dynamically generated and decoupled from the overall size of the box. If the latter picture can be confirmed we would have to blame cooling (or the cooling action we have used) for artificially driving all semiclassical configurations into integer-charged topological lumps at lower temperatures whereas separated monopole constituents are reserved only to higher temperatures. This would explain why previous studies of the topological properties using various cooling (smoothing) techniques (which actually missed the relevant temperature range) were not suitable to discover the non-trivial holonomy accompanying topological charges. In any case, also for $T = 0$ the common instanton interpretation of the QCD vacuum has to be reconsidered.

Acknowledgements

Three of us (E.-M. I., B.V. M. and M. M.-P.) gratefully acknowledge the kind hospitality extended to them at the Instituut-Lorentz of the Universiteit Leiden, where this paper became finalized. We thank Pierre van Baal, Falk Bruckmann, and Christof Gattringer for useful discussions and e-mail correspondence in the final stage of the work. This work was partly supported by RFBR grants 02-02-17308 and 03-02-16941, DFG grant 436 RUS 113/739/0 and RFBR-DFG grant 03-02-04016, by Federal Program of the Russian Ministry of Industry, Science and Technology No 40.052.1.1.1112. Two of us (B.V.M. and A.I.V.) gratefully appreciate the support of Humboldt-University Berlin where this work was initiated and carried out to a large extent. The work of E.-M. I. at Humboldt-University is supported by DFG (FOR 465).

References

- [1] T. C. Kraan and P. van Baal, Phys. Lett. **B435** (1998) 389.
- [2] T. C. Kraan and P. van Baal, Nucl. Phys. **B533** (1998) 627.
- [3] E.-M. Ilgenfritz, M. Müller-Preussker, and A. I. Veselov, in: Proceedings of the NATO Advanced Research Workshop on Lattice Fermions and Structure of the Vacuum, Dubna, Russia, 5 - 9 October 1999, V. K. Mitrjushkin and G. Schierholz (Editors), NATO ASI Series C, Vol. 553, Kluwer Academic, Dordrecht, 2000, p. 345, e-Print Archive: hep-lat/0003025.
- [4] E.-M. Ilgenfritz, B. V. Martemyanov, M. Müller-Preussker, and A. I. Veselov, Nucl. Phys. Proc. Suppl. **94** (2001) 407.

- [5] E.-M. Ilgenfritz, B. V. Martemyanov, M. Müller-Preussker, and A. I. Veselov, Nucl. Phys. Proc. Suppl. **106&107** (2002) 589.
- [6] E.-M. Ilgenfritz, B. V. Martemyanov, M. Müller-Preussker, S. Shcheredin, and A. I. Veselov, Phys. Rev. **D66** (2002) 074503.
- [7] C. Gattringer, Phys. Rev. **D67** (2003) 034507; C. Gattringer and S. Schaefer, Nucl. Phys. **B654** (2003) 30.
- [8] C. Gattringer, E.-M. Ilgenfritz, B. V. Martemyanov, M. Müller-Preussker, D. Peschka, R. Pullirsch, S. Schaefer, and A. Schäfer, presented at *21st International Symposium on Lattice Field Theory (LATTICE 2003)*, Tsukuba, Ibaraki, Japan, 15-19 Jul 2003, e-Print Archive: hep-lat/0309106.
- [9] M. Garcia Perez, A. Gonzalez-Arroyo, A. Montero, and P. van Baal, JHEP **9906** (1999) 001, hep-lat/9903022.
- [10] P. J. Braam and P. van Baal, Comm. Math. Phys. **122** (1989) 267.
- [11] C. Gattringer and R. Pullirsch, *Topological lumps and Dirac zero modes in $SU(3)$ lattice gauge theory on the torus*, hep-lat/0402008.

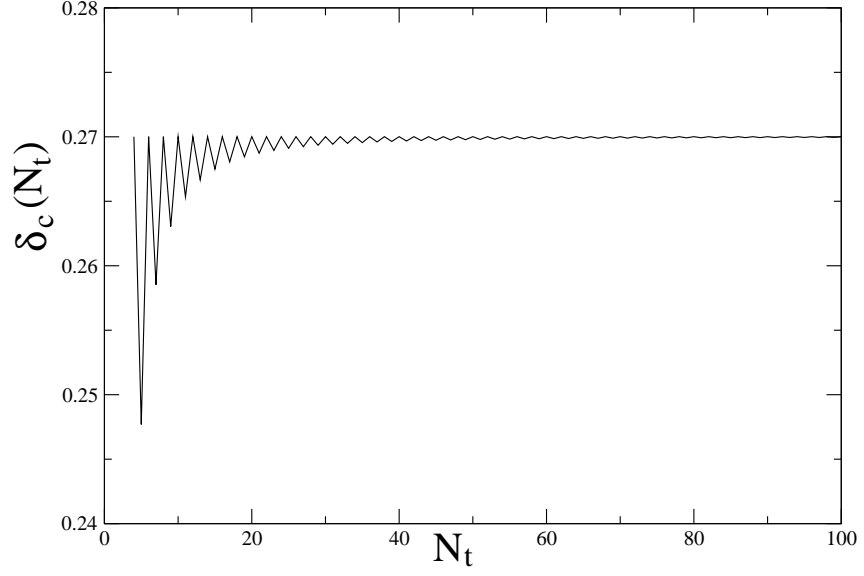


Figure 1: The dependence of non-staticity δ_t^* , defined at the bifurcation point for analytic KvB caloron solutions, on the number of time slices N_t . The zigzag form of the curve can be explained by the qualitatively different arrangement of even and odd time points where the continuum KvB caloron solution has to be calculated in order to evaluate (3).

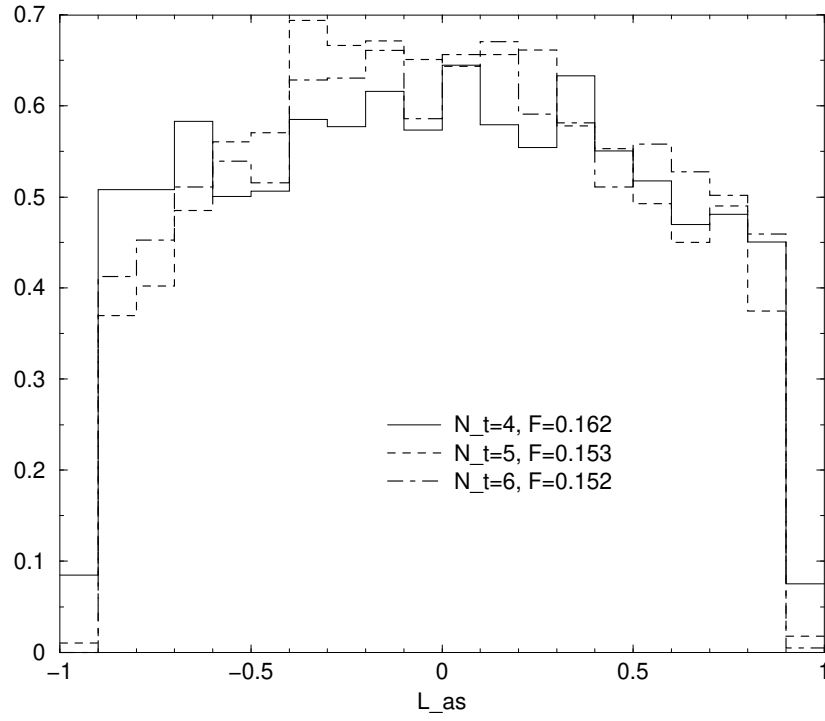


Figure 2: The distribution of holonomy L_{as} for the three samples of cooled configurations corresponding to three temperatures below deconfinement at $N_t = 4$, $N_t = 5$ and $N_t = 6$.

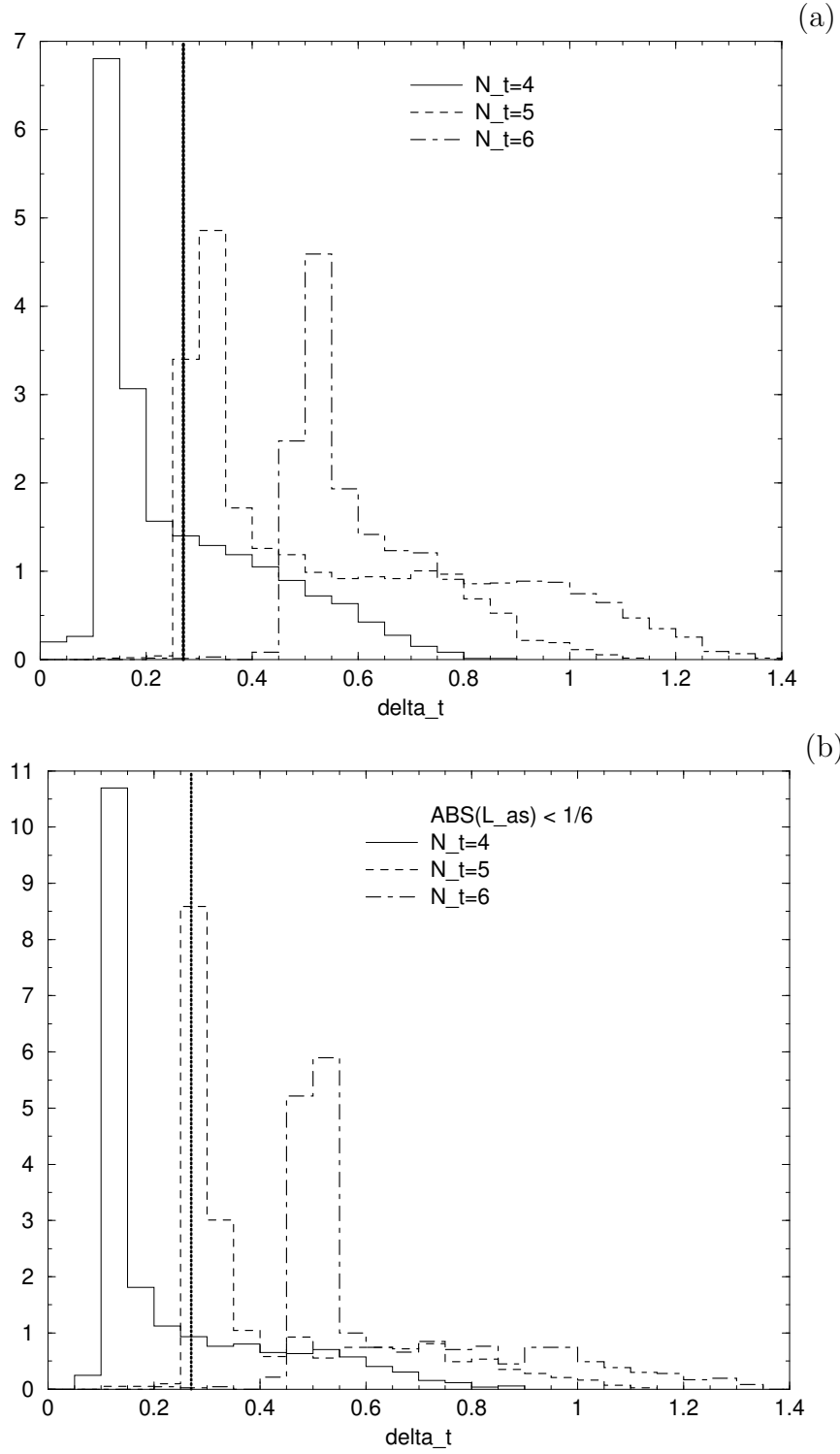


Figure 3: The distribution of non-staticity δ_t after cooling as histograms (with bin width 0.05), for three temperatures below deconfinement at $N_t = 4$, $N_t = 5$ and $N_t = 6$: (a) without any cut, (b) when a cut $|L_{as}| < 1/6$ is applied. The thick vertical line marks the non-staticity δ_t^* where the caloron recombines.

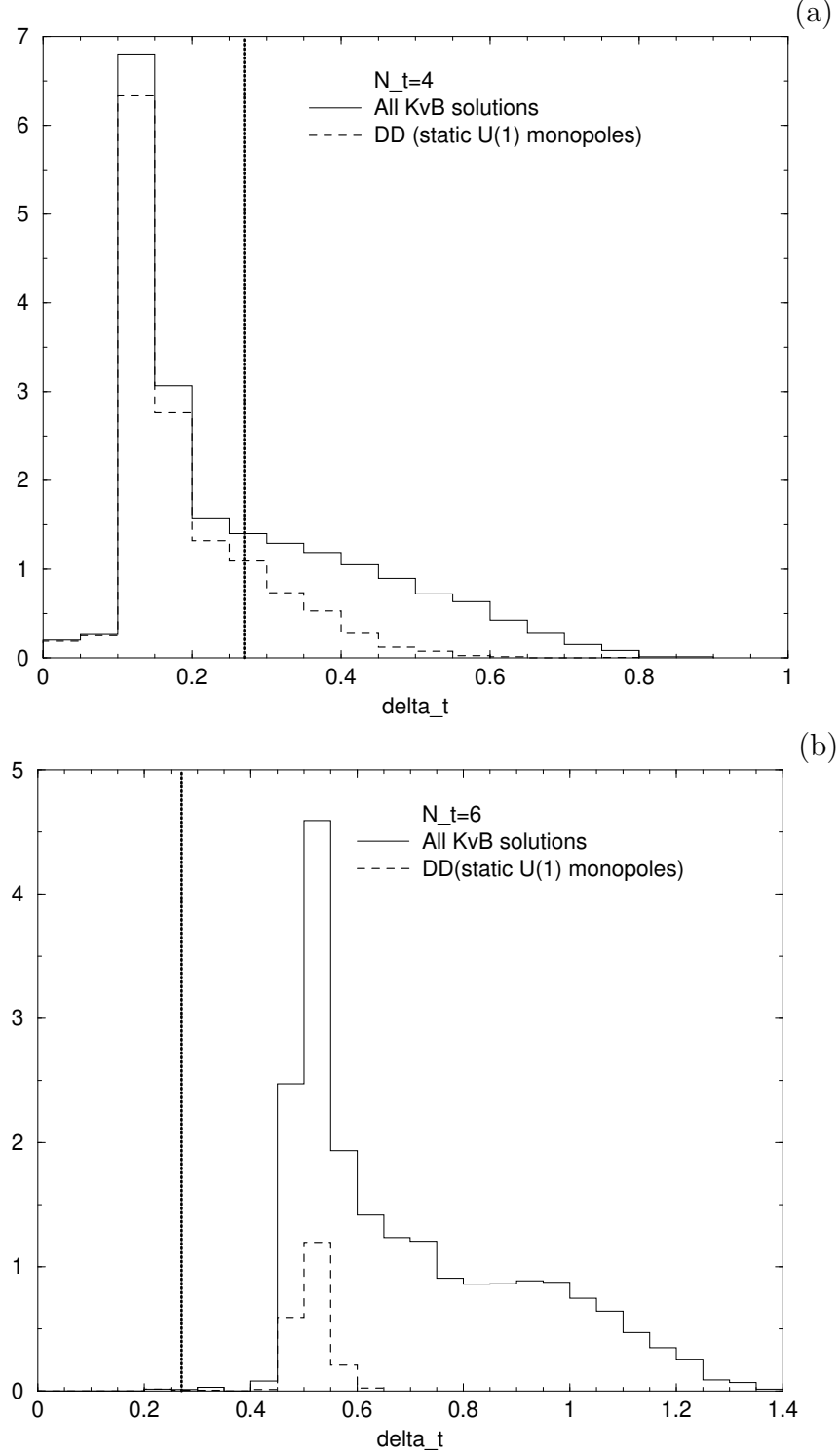


Figure 4: The distribution of non-staticity δ_t after cooling compared with the subsample of configurations which have a static dyon-dyon (DD) structure exhibited by monopoles after Abelian projection: (a) for the higher temperature with $N_t = 4$, (b) for the lower temperature with $N_t = 6$. The thick vertical line marks the non-staticity δ_t^* where the caloron recombines.

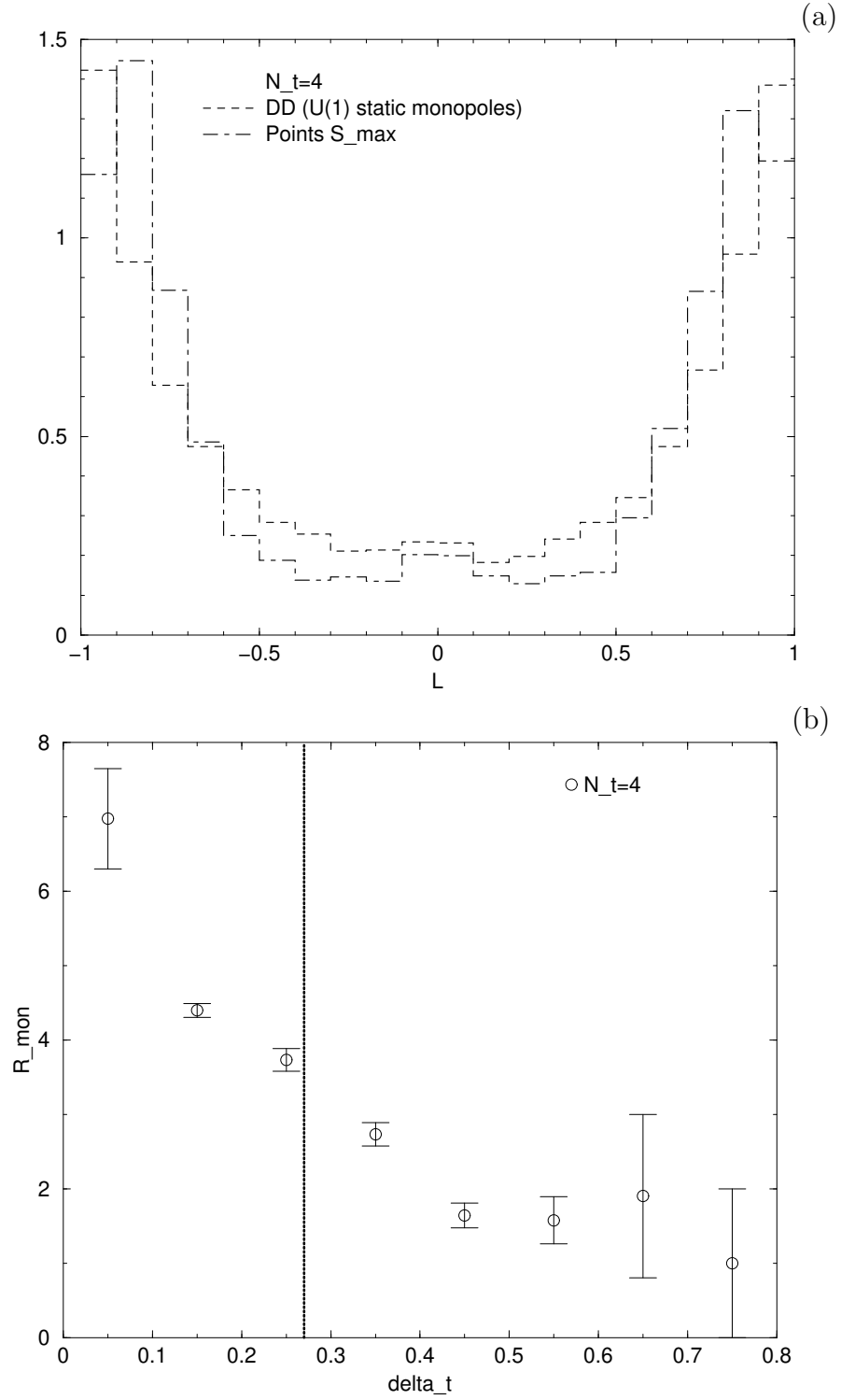


Figure 5: The dyon-dyon structure after Abelian projection : (a) distribution of the local Polyakov loop at the position of the static Abelian monopoles compared to the distribution at the maxima of action density, (b) average distance between the static Abelian monopoles vs. non-staticity δ_t assigned to the cooled configuration. The thick vertical line marks the non-staticity δ_t^* where the caloron recombines.

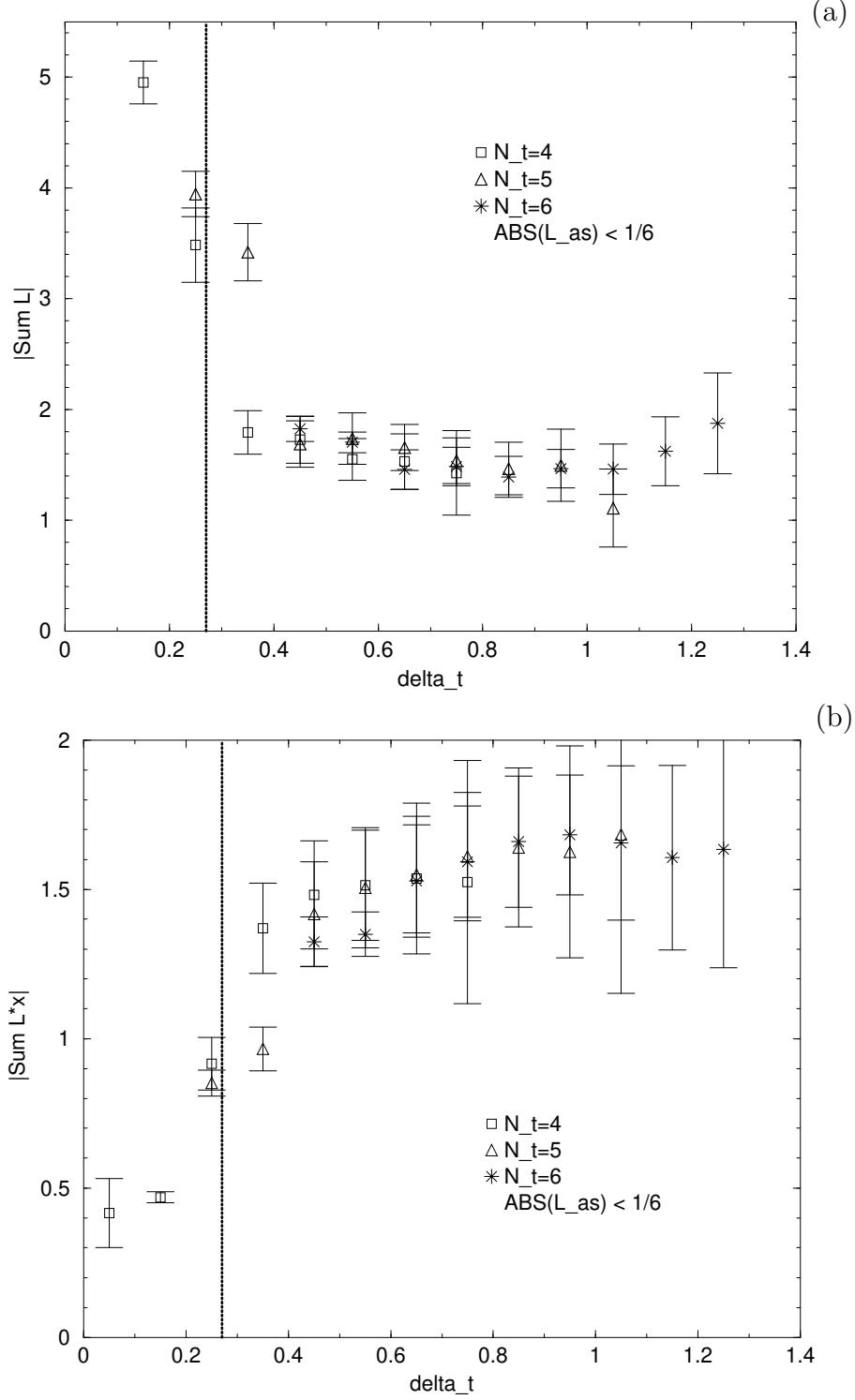


Figure 6: The Polyakov line in the neighborhood of maxima of the action density : (a) modulus of the average summed-up Polyakov line $|L_{\text{tot}}|$ and (b) modulus of the corresponding "dipole moment" $|\vec{M}_{\text{tot}}|$ vs. non-staticity δ_t , for the subsample with asymptotic holonomy near zero. For details of the definition see the text. The thick vertical line marks the non-staticity δ_t^* where the caloron recombines.

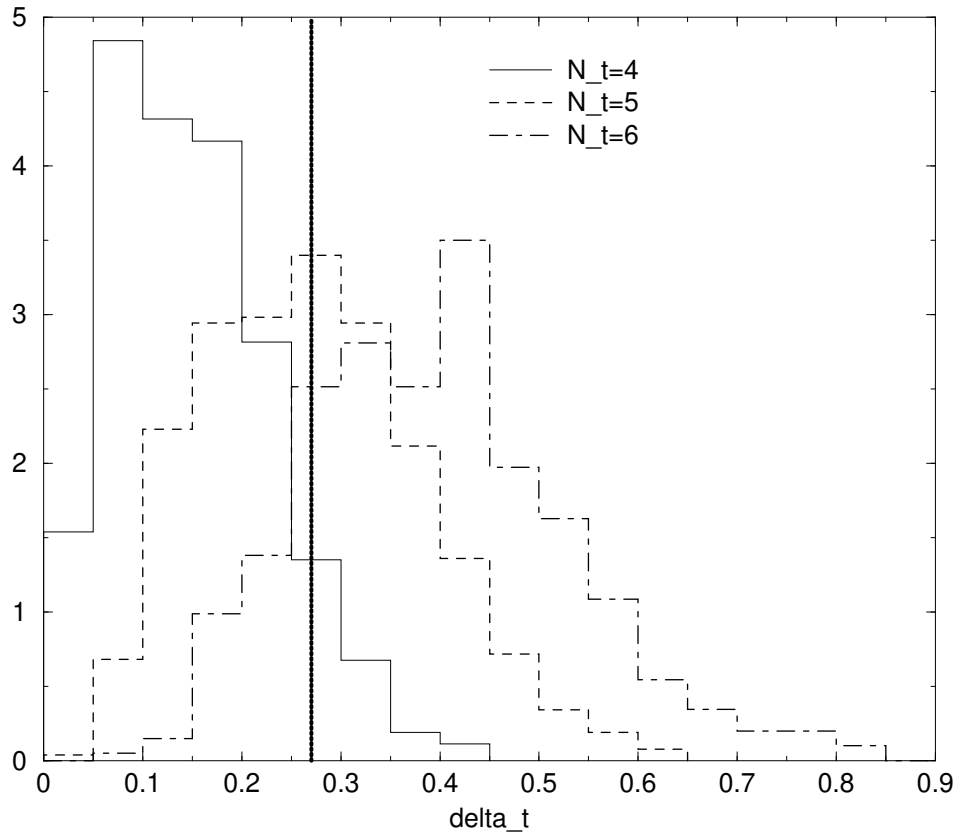


Figure 7: The same as in Fig. 3 (a) for $S = 3S_{inst}$ plateaux. No cut in the asymptotic holonomy has been applied. The thick vertical line marks the non-staticity δ_t^* where the caloron recombines.

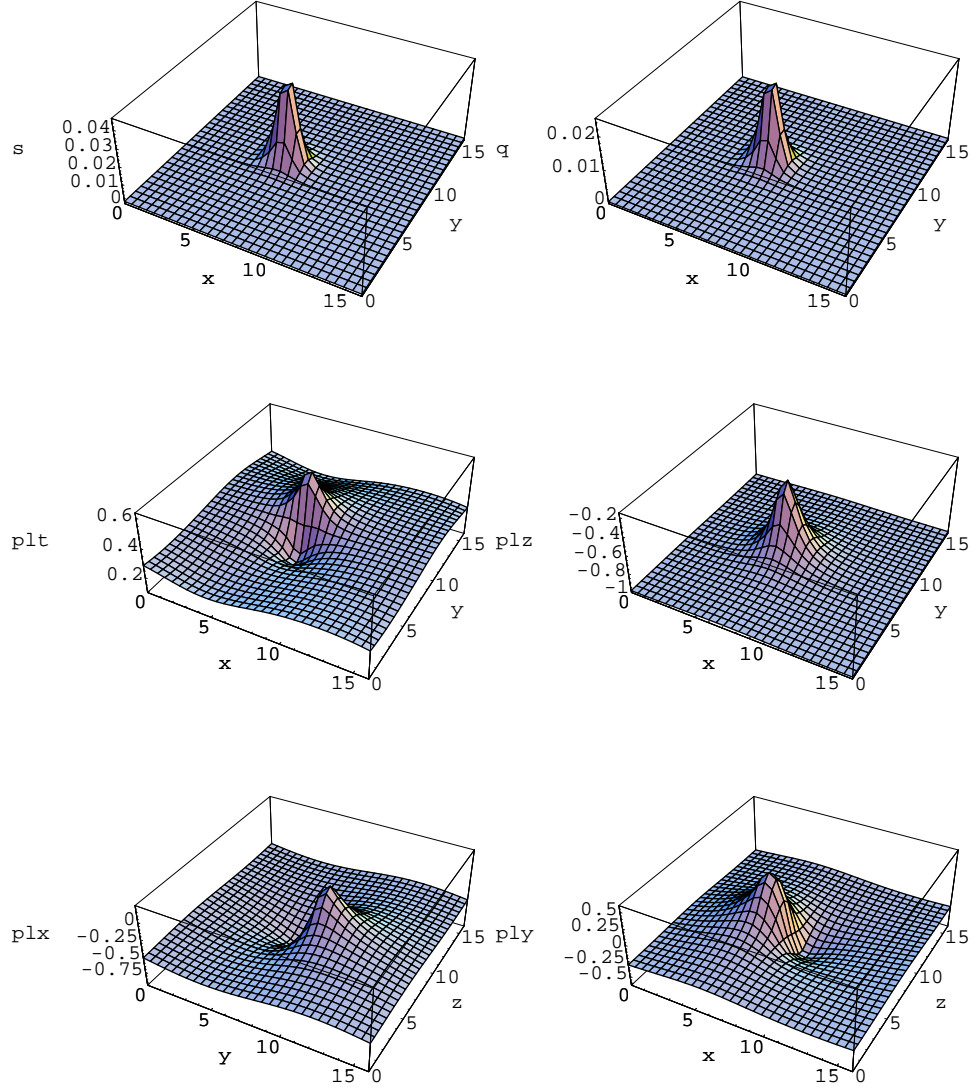


Figure 8: Profiles of the action density (s), the topological charge density (q), and of the Polyakov lines (plt, plx, ply, plz) calculated along all straight line pathes parallel to the four axes for a 16^4 lattice caloron found by cooling a Monte Carlo generated equilibrium gauge field down to the one-instanton action plateau. The center of the caloron (at the maximum of its action density) was found at the site $(x, y, z, t) = (7, 8, 8, 14)$. The planes shown in the figures cross just this point.

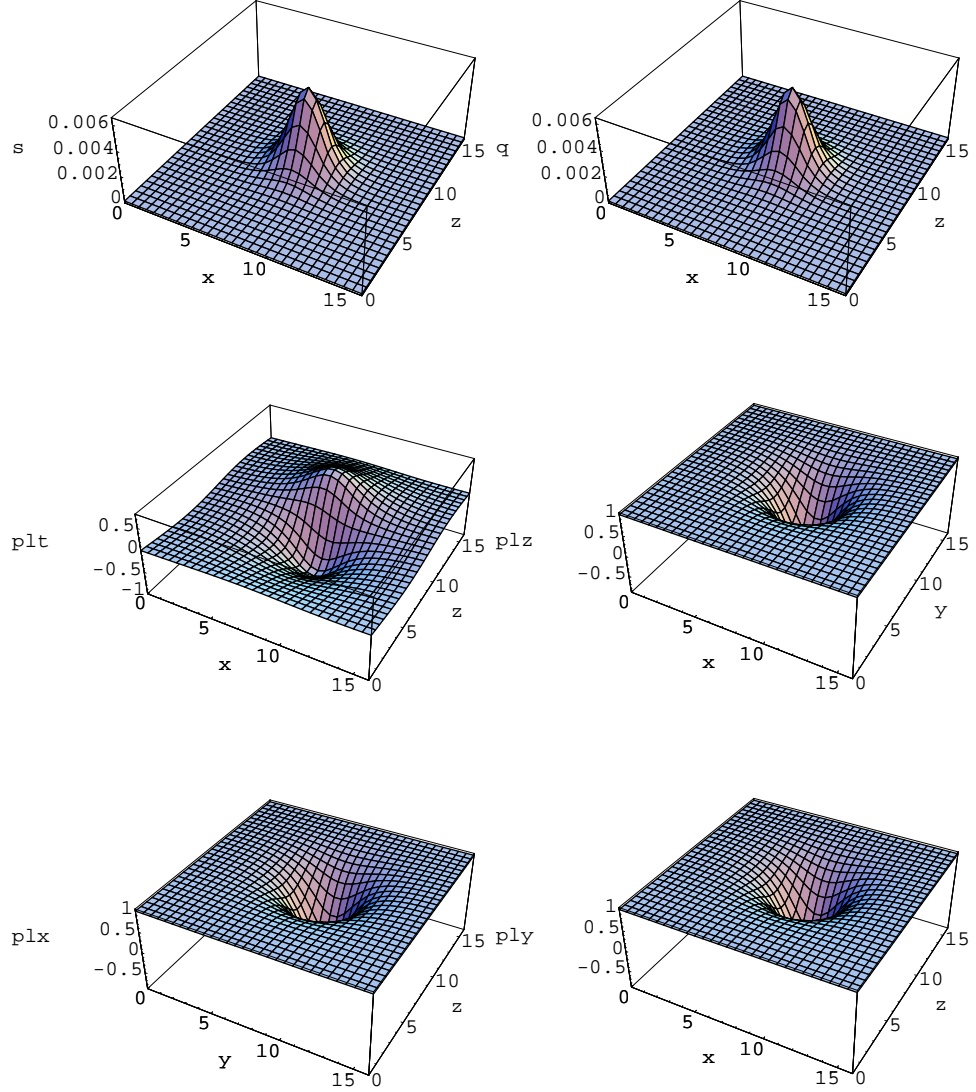


Figure 9: Profiles of the action density (s), the topological charge density (q), and of the Polyakov lines (plt, plx, ply, plz) as in Fig. 8 but for a 16^4 lattice caloron obtained from a discretized KvB solution corrected by some cooling to the one-instanton action plateau (309 cooling steps). The center of the caloron (at the maximum of its action density) was placed to the site $(x, y, z, t) = (8, 8, 8, 1)$. The planes shown in the figures cross this point.